Electromagnetic Transport from Microtearing Mode Turbulence

W. Guttenfelder,[1] J. Candy,[2] S. M. Kaye,[1] W. M. Nevins,[3] E. Wang,[3] R. E. Bell,[1] G. W. Hammett,[1] B. P. LeBlanc,[1] D. R. Mikkelsen,[1] and H. Yuh[4]

[1]*Princeton Plasma Physics Laboratory, Princeton New Jersey 08543, USA*
[2]*General Atomics, San Diego, California 92186, USA*
[3]*Lawrence Livermore National Laboratory, Livermore, California 94551, USA*
[4]*Nova Photonics Inc., Princeton, New Jersey 08540, USA*

(Received 31 December 2010; published 14 April 2011)

This Letter presents nonlinear gyrokinetic simulations of microtearing mode turbulence. The simulations include collisional and electromagnetic effects and use experimental parameters from a high-β discharge in the National Spherical Torus Experiment. The predicted electron thermal transport is comparable to that given by experimental analysis, and it is dominated by the electromagnetic contribution of electrons free-streaming along the resulting stochastic magnetic field line trajectories. Experimental values of flow shear can significantly reduce the predicted transport.

DOI: 10.1103/PhysRevLett.106.155004 PACS numbers: 52.35.Ra, 52.55.Fa, 52.65.Tt

The scaling of normalized energy confinement time with collisionality in spherical tokamaks (STs), $\Omega_i \tau_E \sim \nu_*^{-(0.7-0.9)}$ [1,2], is favorable for extrapolation to next generation devices at lower ν_*. The microtearing mode [3,4] is often predicted to be unstable in neutral beam heated ST experiments [5–7] with a linear growth rate that scales consistent with the measured confinement trends ($\gamma_{\mathrm{lin}} \sim \nu_e$). It is therefore an obvious candidate for describing transport in at least some ST plasmas. This Letter presents first-of-a-kind nonlinear gyrokinetic microtearing mode simulations which predict transport comparable to experimental results in the National Spherical Torus Experiment (NSTX).

Microtearing modes are small scale tearing modes with large toroidal (n) and poloidal (m) mode numbers. Theoretically they are driven unstable by having an electron-temperature gradient (ETG) ∇T_e projected onto helically resonant radial perturbations of magnetic field lines, δB_{mn}, with a rational value of the safety factor, $q = m/n$. The parallel component of ∇T_e can drive a resonant parallel current (which reinforces δB_{mn} via Ampère's law) through multiple mechanisms, such as the (time-dependent) thermal force [3] or interaction between trapped and passing particles [4], both requiring finite collisionality. The existence and strength of the instability will therefore depend on collisionality and electron β (from Ampère's law). In the cylindrical limit, a single resonant mode can reconnect [8] and cause a magnetic island of width $w_{\mathrm{island}} = 4\sqrt{(\delta B/B_0) r R/ns}$ to form, where B_0 is the equilibrium field strength, R (r) is the major (minor) radius, and $s = (r/q)q'$ is the magnetic shear. If the single-mode island width becomes larger than the separation between rational surfaces, $\Delta r_{\mathrm{rat}} = 1/nq' = 1/k_\theta s$ ($k_\theta = nq/r$), stochasticity is expected to develop [9], which can cause rapid transport of electrons following the perturbed field line trajectories [10]. If many toroidal modes are present (separated by Δn), the minimum distance between adjacent resonant surfaces is $\delta r_{\mathrm{rat}} \approx \Delta n/n^2 q'$. Therefore the island overlap criterion for stochasticity onset is more easily satisfied, especially for higher n. Evaluating this condition requires the amplitude of the saturated δB perturbations. The quasilinear approximation $\delta B/B \approx \rho_e/L_{T_e}$ [11] was used along with a collisional test-particle stochastic transport model [10] to model a NSTX discharge, giving quantitative agreement [7]. But the analytic χ_e expression does not follow the scaling of the linear instability, and it is extremely sensitive to T_e and ∇T_e. It is unclear whether these scalings are expected to hold from nonlinear turbulence simulations.

To provide a first-principles prediction of the nonlinear magnetic perturbations δB and corresponding transport, this Letter describes a set of nonlinear gyrokinetic simulations for a discharge in NSTX that is unstable to only the microtearing mode. The simulations require resolving all rational surfaces in the computational domain to achieve saturation, and the transport is almost entirely electromagnetic as a result of stochastic field line trajectories. The predicted electron heat flux is close to experimental levels, illustrating that microtearing turbulence can be important in spherical tokamaks.

The simulations are based on NSTX discharge 120 968 ($B_T = 0.35$ T, $I_p = 0.7$ MA, $P_{\mathrm{NBI}} = 4$ MW, $R/a =$ 0.82 m/0.62 m) that is common to confinement studies that scale plasma current, magnetic field, and dimensionless collisionality and β [1,12]. Linear stability analysis using the Eulerian gyrokinetic code GYRO [13] finds that the microtearing mode is the only ion scale [$k_\theta \rho_s < 1$, where $\rho_s = c_s/\Omega_i$, $c_s = (T_e/m_i)^{1/2}$, $\Omega_i = Z_i eB/m_i$] instability in the outer half radius ($r/a = 0.5$–0.8) while the smaller scale ETG instability ($k_\theta \rho_s \gg 1$) is unstable only farther out ($r/a \approx 0.8$). Figure 1(a) shows that microtearing modes at $r/a = 0.6$ are unstable for $k_\theta \rho_s \leq 1.05$, or $n \leq 50$ ($m \leq 85$, $q = 1.69$). Compressional magnetic

perturbations ($\delta B_\parallel$) have little influence on the growth rate and structure of this mode and are neglected in the nonlinear simulations.

While the microtearing mode in highly shaped, high-β ST plasmas does not always follow more simple theoretical limits [6], gyrokinetic calculations demonstrate the mode requires sufficient β, collisionality, and electron-temperature gradient [$a/L_{T_e} = -(a/T_e)\nabla T_e$] to become linearly unstable. At $r/a = 0.6$ in this NSTX discharge the microtearing mode dominates over all other microinstabilities for a wide range of ν, β, and a/L_{T_e}. This location is therefore ideal for studying pure microtearing mode driven turbulence.

The linear modes exhibit narrow resonant parallel current perturbations ($\delta j_\parallel$) centered on the rational surfaces and almost radially uniform magnetic perturbations. For the most unstable mode at $k_\theta \rho_s = 0.63$ ($n = 30$), the current channel width is $\Delta_j \approx 0.3\rho_s$ or $\sim 1/3$ of the rational surface separation $\Delta r_{\mathrm{rat}} = 0.9\rho_s$ ($s = 1.75$). The corresponding density and potential fluctuations are also narrow and out of phase, very close to an unmagnetized (or adiabatic) ion response, $\delta n/n = -(e\delta\varphi/T)$. As a result of the narrow current channel, fine radial resolution ($\Delta x \approx 0.03\rho_s$) is required to obtain quantitative convergence in the linear growth rate. It is computationally prohibitive (and typically unnecessary) to use such high resolution required for linear convergence in a nonlinear turbulence simulation. However, the microtearing mode depends explicitly on the presence of resonant current perturbations for instability to occur, so it is important to determine the minimum required Δx such that the current channel is resolved for each rational surface. In the present case, for the $n = 30$ mode, this is satisfied for $\Delta x = 0.2\rho_s$. The resulting structure is qualitatively identical to the converged linear result but with a growth rate that is $\sim 15\%$ smaller. Using a coarser resolution ($\Delta x = 0.4\rho_s$) no longer allows for the mode to properly distinguish each rational surface, and the resulting instability takes on a completely different (nonphysical) appearance.

Guided by the discussion above, local nonlinear GYRO simulations were run (with fixed boundary conditions) with perpendicular dimensions $L_x \times L_y = 80 \times 60\rho_s$ using eight complex toroidal modes up to $n = 35$ ($k_\theta \rho_s = 0, 0.105, \ldots, 0.735$) and 400 radial grid points, allowing for all rational surfaces in the simulation domain to be resolved, $\Delta x \approx \min[\Delta r_{\mathrm{rat}}]/4$. All other grid parameters were kept identical to the converged linear calculations, which use numerical equilibrium reconstruction [14] and physical parameters from experimental measurements ($a/L_{T_e} = 2.7$, $a/L_{T_i} = 2.4$, $a/L_n = -0.8$, $T_e/T_i = 1.06$). Two kinetic species are included (electrons and main deuterium ions at full mass ratio, $m_i/m_e = 3600$), with finite electron collisionality ($\nu_{ei} = 1.49 c_s/a$, $Z_{\mathrm{eff}} = 2.9$) and electromagnetic perturbations ($\delta A_\parallel$, $\beta_e = 8\pi n_e T_e/B^2 = 8.8\%$), using 8 energies, 12 pitch angles (2 signs of velocity), and 14 parallel orbit times. The resulting baseline simulation is statistically stationary for a duration longer than $800a/c_s$ (using a time step $\Delta t = 0.002a/c_s$), with no indication of numerical instability. An important verification that these nonlinear simulations are in fact sufficiently resolved is shown by the monotonically decaying tail in the density radial wave number power spectra shown in Fig. 1(b) (integrated over k_θ and averaged over the last $500a/c_s$). Conversely, with half the radial resolution ($\Delta x = 0.4 r_s$), the power spectra for δn (and $\delta j_\parallel$) have the nonphysical appearance of being severely aliased (similar to unpublished simulations [15] using the gyrokinetic code GS2 [16]), and the resulting transport is about 5 times larger. The dramatic change in nonlinear spectra in Fig. 1(b) supports the linear resolution analysis discussed previously.

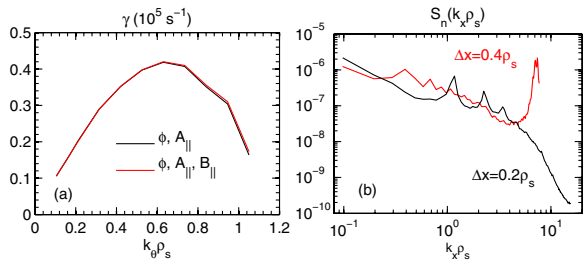

FIG. 1 (color online). (a) Converged linear microtearing spectra with and without compressional magnetic perturbations ($B_\parallel$). (b) Density power spectrum versus k_x for $\Delta x = 0.2\rho_s$ and $0.4\rho_s$.

Consistent with the broad spectra in Fig. 1(b), the density perturbations for the saturated simulation are radially narrow [Fig. 2(a)] and elongated in the poloidal direction, with average correlation lengths $L_x \approx 0.7\rho_s$ and $L_y \approx 4\rho_s$. The structure of the density (and similar potential) perturbations is in stark contrast to the larger, isotropic density structures present in ion scale ion-temperature gradient (ITG) or TEM turbulence ($L_x \approx L_y \approx 7\rho_s$) or the radially elongated eddies at much smaller dimension in ETG turbulence ($L_x/3 \approx L_y \approx 0.15\rho_s$). On the other hand, the magnetic perturbations ($\delta A_\parallel$) are very broad with some instantaneous eddies stretching across the entire simulation domain [Fig. 2(b)].

We emphasize that the narrow radial extent of the density perturbations is largely a remnant of the underlying microtearing mode structure, even though the nonlinearly generated $n = 0$ zonal flows [17] exhibit an average rms zonal flow shear rate, $\langle \omega_s^2 \rangle_{x,t}^{1/2} \approx 0.8 c_s/a$

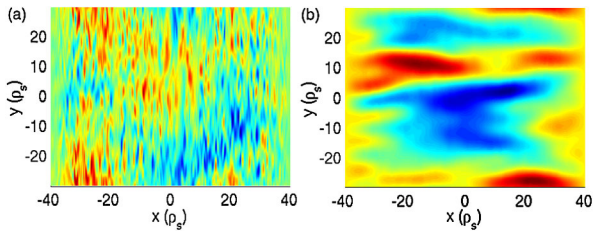

FIG. 2 (color online). Contour plots of (a) δn and (b) $\delta A_\parallel$ perturbations at a snapshot in time.

$[\omega_s = (1/B)d^2(\delta\varphi)/dx^2]$ comparable to the decorrelation rate of the electrostatic perturbations ($\Delta\omega_\varphi \approx 0.6c_s/a$). We also note that the perturbed magnetic shear resulting from the zonal $A_\parallel$ perturbations $[\tilde{s} = (qR/B)d(\delta B_y)/dx]$ [18] is relatively small, $\langle\tilde{s}^2\rangle^{1/2}_{x,t} \approx 0.1$, compared to the equilibrium magnetic shear ($s = 1.75$), and is therefore not expected to be important in the saturation process. For reference, the average rms intensities of nonzonal components ($n > 0$) are approximately $\delta n/n \approx e\varphi/T_e \approx 0.6\%$ and $\delta A_\parallel/c_s T_e \approx 0.4\%$.

The predicted electron thermal diffusivity in gyro-Bohm units is $\chi_e \approx 1.2\rho_s^2 c_s/a$, corresponding to $\chi_e = 6\ \mathrm{m}^2/\mathrm{s}$. This is within the uncertainty of the experimental value $\chi_{e,\mathrm{expt}} \approx 5$–$8\ \mathrm{m}^2/\mathrm{s}$ [1,12], confirming that microtearing mode driven turbulence can indeed cause significant electron thermal transport in NSTX. A unique feature of this simulation is that the electron heat flux is dominated entirely by the electromagnetic "flutter" component ($\chi_{e,\mathrm{em}}/\chi_{e,\mathrm{tot}} > 98\%$). Again, this is in contrast to almost all other published gyrokinetic turbulence simulations, with the exception of cases very near the ideal or kinetic ballooning mode thresholds where $\chi_{e,\mathrm{em}}/\chi_{e,\mathrm{tot}}$ can reach values of 50%–90% [18–20]. As discussed in the introduction, the transport from microtearing modes is expected to be a consequence of island overlap leading to stochastic field line trajectories. To test this, we compare the island widths estimated using the saturated magnetic spectra, $w_{\mathrm{island}} \sim (\delta B_r/n)^{1/2} \sim \delta A_\parallel^{1/2}$, with the minimum separation in rational surfaces, δr_{rat}. Figure 3 shows that the island overlap criteria $w_{\mathrm{island}}(n) > \delta r_{\mathrm{rat}}(n; \Delta n = 5)$ [9] is satisfied above $k_\theta\rho_s > 0.21$ $(n > 10)$, approaching $w_{\mathrm{island}}/\delta r_{\mathrm{rat}} = 8$ at the highest toroidal mode number. As a result, the perturbed field line trajectories are stochastic throughout the entire simulation domain, illustrated by Poincaré surface-of-section plots [21]. Following Rechester and Rosenbluth [10] a magnetic diffusivity

$$D_m = \frac{1}{N}\sum_{i=1}^{N}\lim_{\ell\to\infty}\frac{[r_i(\ell) - r_i(0)]^2}{2\ell} \qquad (1)$$

is calculated [21] to be $D_m = 6\times10^{-7}$ m from an ensemble of $N = 100$ perturbed trajectories, $r_i(\ell)$, integrated for 3000 poloidal transits. As the electron mean free path ($\lambda_{\mathrm{MFP}} = 12.5$ m) is much longer than the magnetic correlation length [10], $L_c = \pi R/\ln(0.5\pi s) \approx 2.5$ m, a collisionless stochastic transport estimate can be made using the model equation $\chi_{e,st} = 2\sqrt{2/\pi}f_p D_m v_{T_e}$ [10,21,22], where $v_{T_e} = (T_e/m_e)^{1/2}$ and $f_p = 63\%$ is the fraction of passing particles expected to follow the perturbed trajectories. The use of f_p is validated by the fact that >70% of the calculated transport comes from passing particles, mostly with energy $E > 2T_e$, i.e., particles with the largest parallel velocity. The resulting model prediction, $\chi_{e,st} = 0.92\rho_s^2 c_s/a$, is within 25% of the simulation, providing strong evidence that the transport is dominated by electrons diffusing in a stochastic magnetic field.

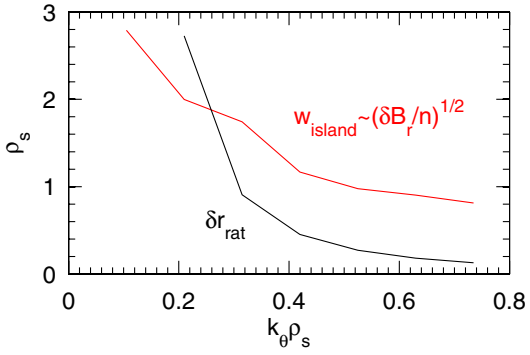

FIG. 3 (color online). Predicted island width at saturation and minimum separation of rational surfaces.

As indicated by the island widths in Fig. 3, the $\delta A_\parallel$ spectrum peaks at the lowest finite $k_\theta\rho_s$ modes. The peak in transport coincides with these modes and is noticeably down-shifted to wavelengths longer than the maximum linear growth rate, $(k_\theta\rho_s)_{\mathrm{lin,max}} = 0.63$ [Fig. 1(a)], as predicted to occur in the nonlinear theory of Drake *et al.* [11]. This theory also predicts a saturated amplitude $\delta B_r/B = \rho_e/L_{T_e} = 0.065\%$, within a factor of ~2 of the simulation result ($\delta B_r/B = 0.15\%$), partially validating the transport model utilized in previous NSTX transport modeling [7]. The fact that the magnetic fluctuations are strongest at the lowest finite toroidal modes is also apparent in the density spectra in Fig. 1(b) where enhanced fluctuations occur around narrow spikes centered at $k_x = 2\pi/\Delta r_{\mathrm{rat}}$ for $n = 5, 10, 15$.

As noted previously, microtearing modes require the electron-temperature gradient to surpass a threshold for instability to occur [7]. The linear threshold for the case here occurs at $a/L_{T_e,\mathrm{th}} \approx 1.5$, well below the experimental gradient, $a/L_{Te,\mathrm{expt}} \approx 2.7$. Figure 4 shows that the predicted transport is very "stiff," increasing 100% for an increase in a/L_{T_e} of 20%, and approaching zero for a 20% reduction. This stiffness suggests that, in locations where microtearing turbulence is active and dominant, profiles should adjust to be near marginal stability. Surprisingly, an effective nonlinear threshold ($a/L_{T_e,\mathrm{NL}} \approx 2.1$) is apparent that is 40% higher than the linear threshold, reminiscent of the so-called "Dimits shift" in ITG turbulence [23]. Such a strong up-shift has been observed before in finite-β ($\beta_e \leq 1\%$) simulations of ITG turbulence [18], although the reason for this remains unclear.

The above simulations do not include the finite toroidal flow and flow shear present in the neutral beam heated NSTX plasma. At $r/a = 0.6$ the $E\times B$ shear rate, γ_E (defined in [24]), is comparable to the maximum linear growth rate of the microtearing modes, $\gamma_{E,\mathrm{expt}}/\gamma_{\mathrm{lin,max}} \approx 1.0$. Previous nonlinear simulations predict complete suppression of ITG and TEM turbulence for $\gamma_E/\gamma_{\mathrm{lin,max}} \approx 1$–2, depending on shaping and other parameters [25]. Unsurprisingly, the microtearing mode turbulence is largely suppressed when restarting the baseline

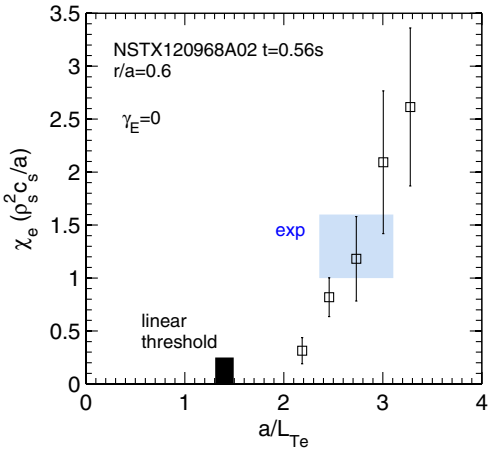

FIG. 4 (color online). Electron thermal transport versus electron-temperature gradient. Vertical bars represent statistical variation in the time-averaged transport. The shaded region represents the range of experimental uncertainty for χ_e and a/L_{T_e}.

simulation with the experimental value of γ_E. While this is now inconsistent with the experimental transport analysis at this location, the dependence in Fig. 4 suggests that only a small increase in a/L_{T_e} may be required to recover significant transport.

It is of great interest to measure turbulence characteristics in an attempt to correlate with the simulated microtearing expectations. Polarimetry measurements have been implemented in other tokamaks to measure δB fluctuations, and a system is being designed that may be sensitive to low-n δB perturbations in NSTX [26]. That the corresponding density perturbations at large poloidal wavelengths ($k_\theta \rho_s \leq 1$) are so narrow ($k_r \rho_s > 1$) (Figs. 1 and 2) also implies they may be detectable by the high-k coherent scattering diagnostic presently implemented on NSTX [27]. Regarding transport, the predicted ion thermal transport is negligible, expected for much slower ions in a stochastic magnetic field, and consistent with the experimental observation that χ_i is well described by neoclassical theory [1]. On the other hand, the stochastic field may contribute to the transport and redistribution of fast ions [28] present from neutral beam heating with large energies ($E_{i,\mathrm{fast}}/T_e > 50$). Additional simulations are required to predict such transport from first principles.

In summary, this Letter presents first-of-a-kind nonlinear microtearing mode simulations using comprehensive gyrokinetic simulations based on a NSTX discharge. The simulations require resolving all rational surfaces to achieve saturation, and the transport is almost entirely electromagnetic as a result of electrons diffusing in the stochastic magnetic field. The resulting electron thermal transport is comparable to experimental analysis, indicating that microtearing modes can indeed cause significant transport in spherical tokamaks.

We gratefully acknowledge generous allocations at NERSC and resources of the Oak Ridge Leadership Computing Facility, supported by DOE Contract No. DE-AC05-00OR22725. This work was also supported by DOE Contracts No. DE-AC02-09CH11466, No. DE-FG03-95ER54309, and No. DE-AC52-07NA27344.

[1] S. M. Kaye *et al.*, Nucl. Fusion **47**, 499 (2007).
[2] M. Valovič *et al.*, in Proceedings of the 23rd IAEA Fusion Energy Conference, Daejon, 2010, p. EXC/P8-18 [Nucl. Fusion (to be published)].
[3] J. F. Drake and Y. C. Lee, Phys. Fluids **20**, 1341 (1977); A. B. Hassam, Phys. Fluids **23**, 2493 (1980).
[4] J. W. Connor, S. C. Cowley, and R. J. Hastie, Plasma Phys. Controlled Fusion **32**, 799 (1990).
[5] F. M. Levinton *et al.*, Phys. Plasmas **14**, 056119 (2007).
[6] D. J. Applegate *et al.*, Plasma Phys. Controlled Fusion **49**, 1113 (2007).
[7] K. L. Wong *et al.*, Phys. Rev. Lett. **99**, 135003 (2007); K. L. Wong *et al.*, Phys. Plasmas **15**, 056108 (2008).
[8] J. Wesson, *Tokamaks* (Oxford University Press, New York, 2004).
[9] G. M. Zaslavsky and B. V. Chirikov, Sov. Phys. Usp. **14**, 549 (1972).
[10] A. B. Rechester and M. N. Rosenbluth, Phys. Rev. Lett. **40**, 38 (1978).
[11] J. F. Drake, N. T. Gladd, C. S. Liu, and C. L. Chang, Phys. Rev. Lett. **44**, 994 (1980).
[12] S. M. Kaye *et al.*, Phys. Rev. Lett. **98**, 175002 (2007).
[13] J. Candy and R. E. Waltz, Phys. Rev. Lett. **91**, 045001 (2003); J. Candy and R. E. Waltz, J. Comput. Phys. **186**, 545 (2003).
[14] J. Candy, Plasma Phys. Controlled Fusion **51**, 105009 (2009).
[15] D. Applegate, Ph.D. thesis, Imperial College London, 2006.
[16] M. Kotschenreuther, G. Rewoldt, and W. M. Tang, Comput. Phys. Commun. **88**, 128 (1995).
[17] P. H. Diamond, S.-I. Itoh, K. Itoh, and T. S. Hahm, Plasma Phys. Controlled Fusion **47**, R35 (2005).
[18] M. J. Pueschel, M. Kammerer, and F. Jenko, Phys. Plasmas **15**, 102310 (2008); M. J. Pueschel and F. Jenko, Phys. Plasmas **17**, 062307 (2010).
[19] F. Jenko and W. Dorland, Plasma Phys. Controlled Fusion **43**, A141 (2001).
[20] J. Candy, Phys. Plasmas **12**, 072307 (2005).
[21] E.Wang *et al.*, Phys. Plasmas (to be published); W. M. Nevins, E. Wang, and J. Candy, Phys. Rev. Lett. **106**, 065003 (2011).
[22] R. W. Harvey, M. G. McCoy, J. Y. Hsu, and A. A. Mirin, Phys. Rev. Lett. **47**, 102 (1981).
[23] A. M. Dimits *et al.*, Phys. Plasmas **7**, 969 (2000).
[24] R. E. Waltz and R. L. Miller, Phys. Plasmas **6**, 4265 (1999).
[25] J. E. Kinsey, R. E. Waltz, and J. Candy, Phys. Plasmas **14**, 102306 (2007).
[26] J. Zhang *et al.*, Bull. Am. Phys. Soc. **55**, 45 (2010).
[27] D. R. Smith *et al.*, Rev. Sci. Instrum. **79**, 123501 (2008).
[28] T. Hauff, M. J. Pueschel, T. Dannert, and F. Jenko, Phys. Rev. Lett. **102**, 075004 (2009).